



HAL
open science

New construction of algebro-geometric solutions to the Camassa-Holm equation and their numerical evaluation

Caroline Kalla, Christian Klein

► **To cite this version:**

Caroline Kalla, Christian Klein. New construction of algebro-geometric solutions to the Camassa-Holm equation and their numerical evaluation. 2011. hal-00627156

HAL Id: hal-00627156

<https://hal.science/hal-00627156>

Preprint submitted on 28 Sep 2011

HAL is a multi-disciplinary open access archive for the deposit and dissemination of scientific research documents, whether they are published or not. The documents may come from teaching and research institutions in France or abroad, or from public or private research centers.

L'archive ouverte pluridisciplinaire **HAL**, est destinée au dépôt et à la diffusion de documents scientifiques de niveau recherche, publiés ou non, émanant des établissements d'enseignement et de recherche français ou étrangers, des laboratoires publics ou privés.

NEW CONSTRUCTION OF ALGEBRO-GEOMETRIC SOLUTIONS TO THE CAMASSA-HOLM EQUATION AND THEIR NUMERICAL EVALUATION

C. KALLA AND C. KLEIN

ABSTRACT. An independent derivation of solutions to the Camassa-Holm equation in terms of multi-dimensional theta functions is presented using an approach based on Fay's identities. Reality and smoothness conditions are studied for these solutions from the point of view of the topology of the underlying real hyperelliptic surface. The solutions are studied numerically for concrete examples, also in the limit where the surface degenerates to the Riemann sphere, and where solitons and cuspons appear.

1. INTRODUCTION

The Camassa-Holm (CH) equation

$$(1.1) \quad u_t + 3uu_x = u_{xxt} + 2u_xu_{xx} + uu_{xxx} - 2k u_x,$$

was first found by Fokas and Fuchssteiner [19] with the method of recursion operators and shown to be a bi-hamiltonian equation with an infinite number of conserved functionals. Camassa and Holm [12] showed that it appeared as a model for unidirectional propagation of waves in shallow water, $u(x, t)$ representing the height of the free surface about a flat bottom, k being a constant related to the critical shallow water speed. In this context, only real-valued solutions are physically meaningful.

To be able to formulate a Cauchy problem for the CH equation which implies the solution of (1.1) for a given function $u(x, 0)$, it is convenient to write (1.1) in the non-local evolutionary form,

$$(1.2) \quad u_t = D^{-1}(-3uu_x + 2u_xu_{xx} + uu_{xxx} - 2k u_x),$$

where the operator D is given by $D = 1 - \partial_{xx}$, and where its inverse is defined by giving certain boundary conditions. This non-locality has mathematically interesting consequences: the CH equation has traveling wave solutions of the form $u(x, t) = c \exp\{-|x - vt|\}$ (v being the speed) called peakons that have a discontinuous first derivative at the wave peak. In particular, Camassa and Holm [12] described the dynamics of the peakons in terms of a finite-dimensional completely integrable Hamiltonian system, namely, each peakon solution is associated with a mechanical system of moving particles. The class of mechanical systems of this type was further extended by Calogero and Françoise in [9, 10]. Multi-peakon solutions were studied using different approaches in a series of papers [4, 5, 6, 11]. Periodic solutions of the shallow water equation were discussed in [26].

A further consequence of this non-locality is that almost periodic solutions of the CH equation in terms of multi-dimensional theta functions do not depend explicitly on the physical coordinates. Such solutions were first given by Alber and Fedorov in [2] by solving a generalized Jacobi inversion problem. In contrast to the well known cases of Korteweg-de Vries (KdV), nonlinear Schrödinger and sine-Gordon equations, see for instance [7] and

references therein, complex solutions of the CH equation are not meromorphic functions of (x, t) but have several branches. This is due to the presence of an implicit function $y(x, t)$ of the variables x and t in the argument of the theta function appearing in the solutions. This monodromy effect is present in the profile of real-valued solutions such as cusps and peakons. This means that even bounded solutions to the CH equation can have discontinuous or infinite derivatives in contrast to KdV solutions. Algebro-geometric solutions of the Camassa-Holm equation and their properties are studied in [1, 2, 3].

Our goal in this paper is to give an independent derivation of such solutions based on identities between multi-dimensional theta functions, which naturally arise from Fay's identity [18]. While the authors in [1, 2, 3] employ the trace formula for the function u in terms of (projections of) auxiliary divisors, and used generalized theta functions and generalized Jacobians (going back to investigations of Clebsch and Gordan [15]), we derive our solutions from a purely transcendental identity satisfied by theta functions. This fits into the program formulated by Mumford [27] that all algebro-geometric solutions to integrable equations should be obtained from Fay's identity and suitable degenerations thereof. This approach was recently successfully in [24, 25] to the multi-component non-linear Schrodinger equations and the Davey-Stewartson equations. We provide here the first example for an integrable equation with nonlocal terms (1.2). The spectral data for these solutions consist of a hyperelliptic curve of the form $\mu^2 = \prod_{j=1}^{2g+2} (\lambda - \lambda_j)$ with three marked points: two of them are interchanged under the involution $\sigma(\lambda, \mu) = (\lambda, -\mu)$, and the third is a ramification point $(\lambda_{j_0}, 0)$.

Our construction of real valued solutions is based on the description of the real and imaginary part of the Jacobian associated to a real hyperelliptic curve (i.e., the branch points λ_j are real or pairwise conjugate non-real). In this way, one gets purely transcendental conditions on the parameters (i.e., without reference to a divisor defined by the solution of a Jacobi inversion problem), such that the solutions are real-valued and smooth. It turns out that continuous real valued solutions are either smooth or have an infinite number of cusp-type singularities.

Concrete examples for the resulting solutions are studied numerically by using the code for real hyperelliptic surfaces [20, 21]. This code uses so-called spectral methods to compute periods on the surfaces. It allows also to study numerically almost degenerate surfaces where the branch points collapse pairwise. In this limit, the theta functions break down to elementary functions, and the solutions describe solitons or cusps. The quality of the numerics is ensured by testing the identities between theta functions which are used to construct the CH solutions in this paper. In addition, the solutions are computed on a grid and are numerically differentiated. These independent tests ensure that the shown solutions are correct to much better than plotting accuracy.

The paper is organized as follows: in section 2 we summarize important facts on Riemann surfaces, especially Fay's identities for theta functions and results on real surfaces. In section 3 we use Fay's identities to rederive theta-functional solutions to the CH equation, and give reality and smoothness conditions. In section 4 we study numerically concrete examples, also in almost degenerate situations. We add some concluding remarks in section 5.

2. THETA FUNCTIONS AND REAL RIEMANN SURFACES

In this section we recall basic facts on Riemann surfaces, in particular real surfaces and multi-dimensional theta functions defined on them.

2.1. **Theta functions.** Let \mathcal{R}_g be a compact Riemann surface of genus $g > 0$. Denote by $(\mathcal{A}, \mathcal{B}) := (\mathcal{A}_1, \dots, \mathcal{A}_g, \mathcal{B}_1, \dots, \mathcal{B}_g)$ a canonical homology basis, and by $(\omega_1, \dots, \omega_g)$ the basis of holomorphic differentials normalized via

$$(2.1) \quad \int_{\mathcal{A}_k} \omega_j = 2i\pi\delta_{kj}, \quad k, j = 1, \dots, g.$$

The matrix $\mathbb{B} = \left(\int_{\mathcal{B}_k} \omega_j \right)$ of \mathcal{B} -periods of the normalized holomorphic differentials ω_j , $j = 1, \dots, g$, is symmetric and has a negative definite real part. The theta function with (half integer) characteristic $\delta = [\delta_1, \delta_2]$ is defined by

$$(2.2) \quad \Theta_{\mathbb{B}}[\delta](\mathbf{z}) = \sum_{\mathbf{m} \in \mathbb{Z}^g} \exp \left\{ \frac{1}{2} \langle \mathbb{B}(\mathbf{m} + \delta_1), \mathbf{m} + \delta_1 \rangle + \langle \mathbf{m} + \delta_1, \mathbf{z} + 2i\pi\delta_2 \rangle \right\},$$

for any $\mathbf{z} \in \mathbb{C}^g$; here $\delta_1, \delta_2 \in \{0, \frac{1}{2}\}^g$ are the vectors of the characteristic δ ; $\langle \cdot, \cdot \rangle$ denotes the scalar product $\langle \mathbf{u}, \mathbf{v} \rangle = \sum_i u_i v_i$ for any $\mathbf{u}, \mathbf{v} \in \mathbb{C}^g$. The theta function $\Theta[\delta](\mathbf{z})$ is even if the characteristic δ is even, i.e., $4 \langle \delta_1, \delta_2 \rangle$ is even, and odd if the characteristic δ is odd i.e., $4 \langle \delta_1, \delta_2 \rangle$ is odd. An even characteristic is called non-singular if $\Theta[\delta](0) \neq 0$, and an odd characteristic is called non-singular if the gradient $\nabla \Theta[\delta](0)$ is non-zero. The theta function with characteristic is related to the theta function with zero characteristic (the Riemann theta function denoted by Θ) as follows

$$(2.3) \quad \Theta[\delta](\mathbf{z}) = \Theta(\mathbf{z} + 2i\pi\delta_2 + \mathbb{B}\delta_1) \exp \left\{ \frac{1}{2} \langle \mathbb{B}\delta_1, \delta_1 \rangle + \langle \mathbf{z} + 2i\pi\delta_2, \delta_1 \rangle \right\}.$$

Denote by Λ the lattice $\Lambda = \{2i\pi\mathbf{N} + \mathbb{B}\mathbf{M}, \mathbf{N}, \mathbf{M} \in \mathbb{Z}^g\}$ generated by the \mathcal{A} and \mathcal{B} -periods of the normalized holomorphic differentials ω_j , $j = 1, \dots, g$. The complex torus $J := J(\mathcal{R}_g) = \mathbb{C}^g / \Lambda$ is called the Jacobian of the Riemann surface \mathcal{R}_g . The theta function (2.2) has the following quasi-periodicity property with respect to the lattice Λ :

$$(2.4) \quad \begin{aligned} & \Theta[\delta](\mathbf{z} + 2i\pi\mathbf{N} + \mathbb{B}\mathbf{M}) \\ &= \Theta[\delta](\mathbf{z}) \exp \left\{ -\frac{1}{2} \langle \mathbb{B}\mathbf{M}, \mathbf{M} \rangle - \langle \mathbf{z}, \mathbf{M} \rangle + 2i\pi(\langle \delta_1, \mathbf{N} \rangle - \langle \delta_2, \mathbf{M} \rangle) \right\}. \end{aligned}$$

Denote by Π the Abel map $\Pi : \mathcal{R}_g \mapsto J$ defined by

$$(2.5) \quad \Pi(p) = \int_{p_0}^p \omega,$$

for any $p \in \mathcal{R}_g$, where $p_0 \in \mathcal{R}_g$ is the base point of the application, and where $\omega = (\omega_1, \dots, \omega_g)^t$ is the vector of the normalized holomorphic differentials. In the whole paper we use the notation $\int_a^b = \Pi(b) - \Pi(a)$.

Now let k_a denote a local parameter near $a \in \mathcal{R}_g$ and consider the following expansion of the normalized holomorphic differentials ω_j , $j = 1, \dots, g$,

$$(2.6) \quad \omega_j(p) = (V_{a,j} + W_{a,j} k_a(p) + \dots) dk_a(p),$$

for any point $p \in \mathcal{R}_g$ in a neighborhood of a , where $V_{a,j}, W_{a,j} \in \mathbb{C}$. Denote by D_a (respectively D'_a) the operator of the directional derivative along the vector $\mathbf{V}_a = (V_{a,1}, \dots, V_{a,g})^t$ (respectively \mathbf{W}_a). According to [27], the theta function satisfies the following identities

derived from Fay's identity [18]:

$$(2.7) \quad D_b \ln \frac{\Theta(\mathbf{z} + f_c^a)}{\Theta(\mathbf{z})} = p_1 + p_2 \frac{\Theta(\mathbf{z} + f_b^a) \Theta(\mathbf{z} + f_c^b)}{\Theta(\mathbf{z} + f_c^a) \Theta(\mathbf{z})},$$

$$(2.8) \quad D_a D_b \ln \Theta(\mathbf{z}) = q_1 + q_2 \frac{\Theta(\mathbf{z} + f_a^b) \Theta(\mathbf{z} - f_a^b)}{\Theta(\mathbf{z})^2},$$

for any $\mathbf{z} \in \mathbb{C}^g$ and any distinct points $a, b \in \mathcal{R}_g$; here the scalars p_i, q_i , $i = 1, 2$ depend on the points a, b and are given by

$$(2.9) \quad p_1(a, b, c) = -D_b \ln \frac{\Theta[\delta](f_a^b)}{\Theta[\delta](f_c^b)},$$

$$(2.10) \quad p_2(a, b, c) = \frac{\Theta[\delta](f_c^a)}{\Theta[\delta](f_b^a) \Theta[\delta](f_b^c)} D_b \Theta[\delta](0),$$

$$(2.11) \quad q_1(a, b) = D_a D_b \ln \Theta[\delta](f_a^b),$$

$$(2.12) \quad q_2(a, b) = \frac{D_a \Theta[\delta](0) D_b \Theta[\delta](0)}{\Theta[\delta](f_a^b)^2},$$

where δ is a non-singular odd characteristic.

2.2. Real Riemann surfaces. A Riemann surface \mathcal{R}_g is called real if it admits an anti-holomorphic involution $\tau : \mathcal{R}_g \rightarrow \mathcal{R}_g$, $\tau^2 = id$. The connected components of the set of fixed points of the anti-involution τ are called real ovals of τ . We denote by $\mathcal{R}_g(\mathbb{R})$ the set of fixed points. According to Harnack's inequality [23], the number χ of real ovals of a real Riemann surface of genus g cannot exceed $g + 1$: $0 \leq \chi \leq g + 1$. Curves with the maximal number $\chi = g + 1$ of real ovals are called M-curves.

The complement $\mathcal{R}_g \setminus \mathcal{R}_g(\mathbb{R})$ has either one or two connected components. The curve \mathcal{R}_g is called a *dividing* curve if $\mathcal{R}_g \setminus \mathcal{R}_g(\mathbb{R})$ has two components, and \mathcal{R}_g is called *non-dividing* if $\mathcal{R}_g \setminus \mathcal{R}_g(\mathbb{R})$ is connected (notice that an M-curve is always a dividing curve).

Example 2.1. Consider the hyperelliptic curve of genus g defined by the equation

$$(2.13) \quad \mu^2 = \prod_{i=1}^{2g+2} (\lambda - \lambda_i),$$

where the branch points $\lambda_i \in \mathbb{R}$ are ordered such that $\lambda_1 < \dots < \lambda_{2g+2}$. On such a curve, we can define two anti-holomorphic involutions τ_1 and τ_2 , given respectively by $\tau_1(\lambda, \mu) = (\bar{\lambda}, \bar{\mu})$ and $\tau_2(\lambda, \mu) = (\bar{\lambda}, -\bar{\mu})$. Projections of real ovals of τ_1 on the λ -plane coincide with the intervals $[\lambda_{2g+2}, \lambda_1], \dots, [\lambda_{2g}, \lambda_{2g+1}]$, whereas projections of real ovals of τ_2 on the λ -plane coincide with the intervals $[\lambda_1, \lambda_2], \dots, [\lambda_{2g+1}, \lambda_{2g+2}]$. Hence the curve (2.13) is an M-curve with respect to both anti-involutions τ_1 and τ_2 .

Let $(\mathcal{A}, \mathcal{B})$ be a basis of the homology group $H_1(\mathcal{R}_g)$. According to Proposition 2.2 in Vinnikov's paper [29] (see also [22]), there exists a canonical homology basis such that

$$(2.14) \quad \begin{pmatrix} \tau \mathcal{A} \\ \tau \mathcal{B} \end{pmatrix} = \begin{pmatrix} \mathbb{I}_g & 0 \\ \mathbb{H} & -\mathbb{I}_g \end{pmatrix} \begin{pmatrix} \mathcal{A} \\ \mathcal{B} \end{pmatrix},$$

where \mathbb{I}_g is the $g \times g$ unit matrix, and \mathbb{H} is a block diagonal $g \times g$ matrix defined as follows:

lifted to the space of differentials: $\tau^*\omega(p) = \omega(\tau p)$ for any $p \in \mathcal{R}_g$. By (2.14) the \mathcal{A} -cycles of the homology basis are invariant under τ . Due to the normalization conditions (2.1), this leads to the following action of τ on the normalized holomorphic differentials:

$$(2.18) \quad \overline{\tau^*\omega_j} = -\omega_j.$$

Let $a, b \in \mathcal{R}_g$ satisfy $\tau a = b$. Using the action (2.15) of τ on the \mathcal{A} -cycles in the homology group $H_1(\mathcal{R}_g \setminus \{a, b\})$, by the uniqueness of the normalized differential of the third kind Ω_{b-a} which has residue 1 at b and residue -1 at a , we get

$$(2.19) \quad \overline{\tau^*\Omega_{b-a}} = -\Omega_{b-a}.$$

Analogously, in the case where $\tau a = a$ and $\tau b = b$, by (2.16) we deduce that

$$(2.20) \quad \overline{\tau^*\Omega_{b-a}} = \Omega_{b-a} + \mathbf{M}^t \omega,$$

where ω denotes the vector of normalized holomorphic differentials. From (2.14) and (2.18) we obtain the following reality property for the Riemann matrix \mathbb{B} :

$$(2.21) \quad \overline{\mathbb{B}} = \mathbb{B} - 2i\pi \mathbb{H}.$$

Moreover, according to Proposition 2.3 in [29], for any $\mathbf{z} \in \mathbb{C}^g$, relation (2.21) implies

$$(2.22) \quad \overline{\Theta(\mathbf{z})} = \kappa \Theta(\bar{\mathbf{z}} - i\pi \text{diag}(\mathbb{H})),$$

where $\text{diag}(\mathbb{H})$ denotes the vector of diagonal elements of the matrix \mathbb{H} , and κ is a root of unity which depends on the matrix \mathbb{H} (knowledge of the exact value of κ is not needed for our purpose).

2.3. Action of τ on the Jacobian and the theta divisor of real Riemann surfaces.

In this part, we review known results about the theta divisor of real Riemann surfaces (see [29, 16]). Let us choose the canonical homology basis satisfying (2.14) and consider the Jacobian $J := J(\mathcal{R}_g)$ of a real Riemann surface \mathcal{R}_g .

The anti-holomorphic involution τ on \mathcal{R}_g gives rise to an anti-holomorphic involution on the Jacobian: if \mathcal{D} is a positive divisor of degree n on \mathcal{R}_g , then $\tau \mathcal{D}$ is the class of the point $(\int_n^{\tau \mathcal{D}} \omega) = (\int_n^{\mathcal{D}} \tau^* \omega)$ in the Jacobian. Therefore, by (2.18) τ lifts to the anti-holomorphic involution on J , denoted also by τ , given by

$$(2.23) \quad \tau \zeta = -\bar{\zeta} + n_\zeta \Pi(\tau p_0),$$

for any $\zeta \in J$, where $n_\zeta \in \mathbb{Z}$, $n_\zeta \leq g$, is the degree of the divisor \mathcal{D} such that $\Pi(\mathcal{D}) = \zeta$.

Now consider the following two subsets of the Jacobian

$$(2.24) \quad S_1 = \{\zeta \in J; \zeta + \tau \zeta = i\pi \text{diag}(\mathbb{H})\},$$

$$(2.25) \quad S_2 = \{\zeta \in J; \zeta - \tau \zeta = i\pi \text{diag}(\mathbb{H})\},$$

where the matrix \mathbb{H} was introduced in (2.14). Below we study their intersections $S_1 \cap (\Theta)$ and $S_2 \cap (\Theta)$ with the theta divisor (Θ) , the set of zeros of the theta function. Let us introduce the notation: $(e_i)_k = \delta_{ik}$, $\mathbb{B}_i = \mathbb{B} e_i$. The following proposition was proved in [29].

Proposition 2.1. *The set S_1 is the disjoint union of the tori T_v defined by*

$$(2.26) \quad T_v = \{\zeta \in J; \zeta = i\pi (\text{diag}(\mathbb{H})/2 + v_1 e_{r+1} + \dots + v_{g-r} e_g) + \beta_1 \text{Re}(\mathbb{B}_1) + \dots + \beta_g \text{Re}(\mathbb{B}_g), \\ \beta_1, \dots, \beta_r \in \mathbb{R}/2\mathbb{Z}, \beta_{r+1}, \dots, \beta_g \in \mathbb{R}/\mathbb{Z}\},$$

where $v = (v_1, \dots, v_{g-r}) \in (\mathbb{Z}/2\mathbb{Z})^{g-r}$ and r is the rank of the matrix \mathbb{H} . Moreover, if $\mathcal{R}_g(\mathbb{R}) \neq \emptyset$, then $T_v \cap (\Theta) = \emptyset$ if and only if the curve is dividing and $v = 0$.

The last statement means that among all curves which admit real ovals, the only torus T_v which does not intersect the theta divisor is the torus T_0 corresponding to dividing curves. This torus is given by

$$(2.27) \quad T_0 = \{\zeta \in J; \zeta = \beta_1 \operatorname{Re}(\mathbb{B}_1) + \dots + \beta_g \operatorname{Re}(\mathbb{B}_g), \beta_1, \dots, \beta_r \in \mathbb{R}/2\mathbb{Z}, \beta_{r+1}, \dots, \beta_g \in \mathbb{R}/\mathbb{Z}\}.$$

It is straightforward to prove that the set S_1 is the disjoint union of the tori (2.26). Moreover, in the case where $\mathcal{R}_g(\mathbb{R}) \neq \emptyset$ and \mathcal{R}_g is non-dividing, for all v the torus T_v contains an odd half-period which yields $T_v \cap (\Theta) \neq \emptyset$. The same holds for all $v \neq 0$ in the case where the curve is dividing or does not have real ovals. Corollary 4.3 in [29] proves that if \mathcal{R}_g is dividing then $T_0 \cap (\Theta) = \emptyset$.

The following proposition was proved in [16].

Proposition 2.2. *The set S_2 is the disjoint union of the tori \tilde{T}_v defined by*

$$(2.28) \quad \tilde{T}_v = \{\zeta \in J; \zeta = 2i\pi(\alpha_1 e_1 + \dots + \alpha_g e_g) + (v_1/2)\mathbb{B}_{r+1} + \dots + (v_{g-r}/2)\mathbb{B}_g, \\ \alpha_1, \dots, \alpha_g \in \mathbb{R}/\mathbb{Z}\},$$

where $v = (v_1, \dots, v_{g-r}) \in (\mathbb{Z}/2\mathbb{Z})^{g-r}$ and r is the rank of the matrix \mathbb{H} . Moreover, if $\mathcal{R}_g(\mathbb{R}) \neq \emptyset$, then $\tilde{T}_v \cap (\Theta) = \emptyset$ if and only if the curve is an M -curve and $v = 0$.

3. ALGEBRO-GEOMETRIC SOLUTIONS OF THE CAMASSA-HOLM EQUATION

In this section we will use Fay's identities to construct solutions to the CH equation on hyperelliptic surfaces. For the resulting formulae we establish conditions to obtain real and smooth solutions. In what follows \mathcal{R}_g denotes a hyperelliptic curve of genus $g > 0$, written as

$$(3.1) \quad \mu^2 = \prod_{i=1}^{2g+2} (\lambda - \lambda_i),$$

where the branch points $\lambda_i \in \mathbb{C}$ satisfy the relations $\lambda_i \neq \lambda_j$ for $i \neq j$. We denote by σ the hyperelliptic involution defined by $\sigma(\lambda, \mu) = (\lambda, -\mu)$. Note that the CH equation can be expressed in the following simple form,

$$(3.2) \quad m_t + u m_x + 2 m u_x = 0,$$

where we put $m := u - u_{xx} + k$.

3.1. Identities between theta functions. In our approach to construct algebro-geometric solutions of the CH equation we use the corollaries (2.7) and (2.8) of Fay's identity.

Proposition 3.1. *Let $a, b \in \mathcal{R}_g$ such that $\sigma(a) = b$ and let $e \in \mathcal{R}_g$ be a ramification point, namely, $e = (\lambda_j, 0)$ for some $j \in \{1, \dots, 2g+2\}$. Denote by g_1 and g_2 the following functions of the variable $\mathbf{z} \in \mathbb{C}^g$:*

$$(3.3) \quad g_1(\mathbf{z}) = \frac{\Theta(\mathbf{z} + \frac{\mathbf{r}}{2})}{\Theta(\mathbf{z})}, \quad g_2(\mathbf{z}) = \frac{\Theta(\mathbf{z} - \frac{\mathbf{r}}{2})}{\Theta(\mathbf{z})},$$

where $\mathbf{r} = \int_a^b \omega$ and ω is the vector of normalized holomorphic differentials. Then the two following identities hold:

$$(3.4) \quad D_b D_e \ln \frac{g_1}{g_2} = -\frac{p_2}{g_1 g_2} D_b \ln g_1 g_2,$$

$$(3.5) \quad D_b D_e \ln(g_1 g_2) = \frac{\tilde{q}_2}{\tilde{p}_2} \frac{1}{g_1 g_2} \left(D_b \ln \frac{g_1}{g_2} - 2\tilde{p}_1 \right) - 2\tilde{q}_2 g_1 g_2.$$

Here we used the notation:

$$(3.6) \quad p_2 = p_2(b, e, a), \quad \tilde{p}_i = p_i(e, b, a), \quad \tilde{q}_2 = q_2(b, e),$$

where the scalars $q_2(\cdot, \cdot)$ and $p_i(\cdot, \cdot, \cdot)$, $i = 1, 2$, are defined in (2.12) and (2.9), (2.10); D_b (respectively D_e) denotes the directional derivative along the vector \mathbf{V}_b (respectively \mathbf{V}_e) defined in (2.6).

Proof. Under the changes of variables $(a, b, c) \rightarrow (b, e, a)$ and $\mathbf{z} \rightarrow \mathbf{z} - \mathbf{r}/2$, identity (2.7) becomes

$$(3.7) \quad D_e \ln \frac{g_1}{g_2} = p_1 + \frac{p_2}{g_1 g_2}.$$

Here we used the fact that $\int_a^e \omega = \int_e^b \omega = \mathbf{r}/2$, according to the action of σ^* (the action of σ lifted to the space of one-forms) on the normalized holomorphic differentials ω_j :

$$(3.8) \quad \sigma^* \omega_j = -\omega_j, \quad j = 1, \dots, g.$$

Applying the differential operator D_b to the equation (3.7) one gets:

$$D_b D_e \ln \frac{g_1}{g_2} = -p_2 \frac{D_b(g_1 g_2)}{(g_1 g_2)^2} = -\frac{p_2}{g_1 g_2} D_b \ln g_1 g_2,$$

which proves (3.4). To prove (3.5), consider the change of variables $(a, b, c) \rightarrow (e, b, a)$ in (2.7), which leads to

$$D_b \ln g_1 = \tilde{p}_1 + \tilde{p}_2 g_2 \frac{\Theta(\mathbf{z} + \mathbf{r})}{\Theta(\mathbf{z} + \frac{\mathbf{r}}{2})}.$$

Changing \mathbf{z} to $-\mathbf{z}$ in the last equality, one gets

$$D_b \ln g_2 = -\tilde{p}_1 - \tilde{p}_2 g_1 \frac{\Theta(\mathbf{z} - \mathbf{r})}{\Theta(\mathbf{z} - \frac{\mathbf{r}}{2})}.$$

From these two identities, it can be deduced that

$$(3.9) \quad \frac{\Theta(\mathbf{z} + \mathbf{r})}{\Theta(\mathbf{z} + \frac{\mathbf{r}}{2})} = (\tilde{p}_2 g_2)^{-1} (D_b \ln g_1 - \tilde{p}_1),$$

$$(3.10) \quad \frac{\Theta(\mathbf{z} - \mathbf{r})}{\Theta(\mathbf{z} - \frac{\mathbf{r}}{2})} = -(\tilde{p}_2 g_1)^{-1} (D_b \ln g_2 + \tilde{p}_1).$$

Moreover, since

$$D_b D_e \ln(g_1 g_2) = D_b D_e \ln \Theta\left(\mathbf{z} + \frac{\mathbf{r}}{2}\right) + D_b D_e \ln \Theta\left(\mathbf{z} - \frac{\mathbf{r}}{2}\right) - 2 D_b D_e \ln \Theta(\mathbf{z}),$$

using (2.8) one gets

$$(3.11) \quad D_b D_e \ln(g_1 g_2) = \frac{\tilde{q}_2}{g_1} \frac{\Theta(\mathbf{z} + \mathbf{r})}{\Theta(\mathbf{z} + \frac{\mathbf{r}}{2})} + \frac{\tilde{q}_2}{g_2} \frac{\Theta(\mathbf{z} - \mathbf{r})}{\Theta(\mathbf{z} - \frac{\mathbf{r}}{2})} - 2\tilde{q}_2 g_1 g_2,$$

which by (3.9) and (3.10) leads to (3.5). \square

With identities (3.4) and (3.5) we are now able to construct theta-functional solutions of the CH equation:

Proposition 3.2. *Let $a, b \in \mathcal{R}_g$ such that $\sigma(a) = b$, and let $e \in \mathcal{R}_g$ be a ramification point. Denote by ℓ an oriented contour between a and b which contains point e . Assume that ℓ does not cross cycles of the canonical homology basis. Choose arbitrary constants $\mathbf{d} \in \mathbb{C}^g$ and $k, \zeta \in \mathbb{C}$. Let $y(x, t)$ be an implicit function of the variables $x, t \in \mathbb{R}$ defined by*

$$(3.12) \quad x + \alpha_1 y + \alpha_2 t + \zeta = \ln \frac{\Theta(\mathbf{Z} - \mathbf{d} + \frac{\mathbf{r}}{2})}{\Theta(\mathbf{Z} - \mathbf{d} - \frac{\mathbf{r}}{2})},$$

where $\mathbf{r} = \int_{\ell} \omega$. Here the vector \mathbf{Z} is given by

$$(3.13) \quad \mathbf{Z}(x, t) = \mathbf{V}_e y(x, t) + \mathbf{V}_b t,$$

where the vectors \mathbf{V}_e and \mathbf{V}_b are defined in (2.6). The scalars α_1 and α_2 satisfy

$$(3.14) \quad \alpha_1 = p_1(b, e, a), \quad \alpha_2 = 2p_1(e, b, a) + k,$$

where the function p_1 is defined in (2.9). Then the following function of the variables x and t is solution of the CH equation:

$$(3.15) \quad u(x, t) = D_b \ln \frac{\Theta(\mathbf{Z} - \mathbf{d} + \frac{\mathbf{r}}{2})}{\Theta(\mathbf{Z} - \mathbf{d} - \frac{\mathbf{r}}{2})} - \alpha_2.$$

Here D_b denotes the directional derivative along the vector \mathbf{V}_b .

Proof. Let $\beta, \delta \in \mathbb{C}$ and $\alpha_1, \alpha_2 \in \mathbb{C}$ be arbitrary constants. Let us look for solutions u of CH having the form

$$(3.16) \quad u(x, t) = \beta D_b \ln \frac{\Theta(\mathbf{Z} - \mathbf{d} + \frac{\mathbf{r}}{2})}{\Theta(\mathbf{Z} - \mathbf{d} - \frac{\mathbf{r}}{2})} + \delta = \beta D_b \ln \frac{g_1}{g_2} + \delta,$$

where $\mathbf{Z}(x, t)$ is defined in (3.13), and the functions g_1, g_2 were introduced in (3.3) with $\mathbf{z} = \mathbf{Z}(x, t) - \mathbf{d}$. By (3.12), the derivative with respect to the variable x of the implicit function $y(x, t)$ is given by

$$y_x = \left(D_e \ln \frac{g_1}{g_2} - \alpha_1 \right)^{-1}.$$

Putting $\alpha_1 = p_1(b, e, a)$, relation (3.7) implies

$$(3.17) \quad y_x = \frac{g_1 g_2}{p_2}.$$

Analogously it can be checked that

$$(3.18) \quad y_t = -y_x \left(\frac{u}{\beta} - \frac{\delta}{\beta} - \alpha_2 \right).$$

Now let us express the function $m(x, t) = u - u_{xx} + k$ introduced in (3.2) in terms of the functions g_1 and g_2 of (3.3). By (3.4) and (3.17), the first derivative of the function u (3.16) with respect to the variable x is given by

$$(3.19) \quad u_x = -\beta D_b \ln(g_1 g_2).$$

By (3.5) and (3.17) we obtain for the second derivative of u with respect to x :

$$(3.20) \quad u_{xx} = \beta \left(D_b \ln \frac{g_1}{g_2} - 2\tilde{p}_1 \right) - 2\beta \tilde{p}_2 (g_1 g_2)^2;$$

here we used the identity $\tilde{q}_2 = -\tilde{p}_2 p_2$ relating the scalars \tilde{q}_2, \tilde{p}_2 and p_2 defined in (3.6). Therefore, with (3.16) and (3.20), the function m reads

$$(3.21) \quad m(x, t) = \delta + k + 2\beta \tilde{p}_1 + 2\beta \tilde{p}_2 (g_1 g_2)^2.$$

Taking the derivative of m with respect to x , and the derivative of m with respect to t , one gets respectively:

$$(3.22) \quad m_x(x, t) = 4\beta \tilde{p}_2 (g_1 g_2)^2 y_x D_e \ln(g_1 g_2),$$

$$(3.23) \quad m_t(x, t) = 4\beta \tilde{p}_2 (g_1 g_2)^2 (y_t D_e \ln(g_1 g_2) + D_b \ln(g_1 g_2)).$$

Therefore, entering with the functions (3.16), (3.19), (3.22) and (3.23) into the CH equation (3.2) we obtain

$$\begin{aligned} & 2\tilde{p}_2 D_e \ln(g_1 g_2) y_x (g_1 g_2)^2 \left[u \left(1 - \frac{1}{\beta} \right) + \frac{\delta}{\beta} + \alpha_2 \right] \\ & - D_b \ln(g_1 g_2) (\delta + k + 2\beta \tilde{p}_1 + 2\tilde{p}_2 (g_1 g_2)^2 (\beta - 1)) = 0. \end{aligned}$$

In particular, the previous equality holds for $\beta = 1$, $\delta = -2\tilde{p}_1 - k$ and $\alpha_2 = -\delta$, which completes the proof. \square

3.2. Real-valued solutions and smoothness conditions. In this part, we identify real-valued and smooth solutions of the CH equation. Assume that \mathcal{R}_g is a real hyperelliptic curve which admits real ovals with respect to an anti-holomorphic involution τ . Let us choose the homology basis satisfying (2.14). Recall that $\mathcal{R}_g(\mathbb{R})$ denotes the set of fixed points of the anti-holomorphic involution τ .

The following propositions provide reality and smoothness conditions for the solutions $u(x, t)$ (3.15) in the case where the points a and b are stable under τ , and in the case where $\tau a = b$. In particular, it is proved that, for fixed $t_0 \in \mathbb{R}$, the function $u(x, t_0)$ is smooth with respect to the real variable x when a and b are stable under τ . In the case where $\tau a = b$, the function $u(x, t_0)$ is either smooth, or it has cusp-like singularities.

Proposition 3.3. *Assume that all ramification points of \mathcal{R}_g are stable under τ and denote by $e \in \mathcal{R}_g(\mathbb{R})$ one of them. Let $a, b \in \mathcal{R}_g(\mathbb{R})$ such that $\sigma(a) = b$. For any $c \in \{a, b, e\}$, choose the local parameter k_c such that $\overline{k_c(\tau p)} = k_c(p)$ for any point p in a neighborhood of c . Denote by ℓ an oriented contour between a and b containing point e , which does not intersect cycles of the canonical homology basis. Choose ℓ such that the closed path $\tau \ell - \ell$ is homologous to zero in $H_1(\mathcal{R}_g)$. Take $\mathbf{d} \in i\mathbb{R}^g$ and $k \in \mathbb{R}$. Choose $\zeta \in \mathbb{C}$ in (3.12) such that $\ln \left(\frac{\Theta(\mathbf{d}+\mathbf{r}/2)}{\Theta(\mathbf{d}-\mathbf{r}/2)} \right) - \zeta$ is real. Then solutions $u(x, t)$ of the CH equation given in (3.15) are real-valued, and for fixed $t_0 \in \mathbb{R}$, the function $u(x, t_0)$ is smooth with respect to the real variable x .*

Proof. Let us check that under the conditions of the proposition, the function $u(x, t)$ (3.15) is real-valued. First of all, invariance with respect to the anti-involution τ of the points e and b implies

$$(3.24) \quad \overline{\mathbf{Z}} = -\mathbf{Z},$$

where the vector \mathbf{Z} is defined in (3.13). In fact, using the expansion (2.6) of the normalized holomorphic differentials ω_j near e (respectively b) one gets

$$\overline{\tau^* \omega_j}(e)(p) = (\overline{V_{e,j}} + \overline{W_{e,j}} k_e(p) + o(k_e(p)^2)) dk_e(p),$$

for any point p in a neighborhood of e (respectively b). Then by (2.18), the vectors \mathbf{V}_e and \mathbf{V}_b appearing in the vector \mathbf{Z} are purely imaginary, which leads to (3.24). Moreover, since the closed contour $\tau\ell - \ell$ is homologous to zero in $H_1(\mathcal{R}_g)$, from (2.18) one gets

$$(3.25) \quad \bar{\mathbf{r}} = -\mathbf{r}.$$

Using the representation in terms of multi-dimensional theta functions of the differential Ω_{c-a} (see, for instance, [7]), one gets:

$$(3.26) \quad \Omega_{c-a}(b) = p_1(a, b, c) dk_b.$$

We deduce that the scalars $p_1(b, e, a)$ and $p_1(e, b, a)$ appearing respectively in α_1 and α_2 (see (3.14)) satisfy

$$(3.27) \quad \Omega_{a-b}(e) = p_1(b, e, a) dk_e, \quad \Omega_{a-e}(b) = p_1(e, b, a) dk_b.$$

Therefore, from (2.20) it can be deduced that $p_1(b, e, a)$ and $p_1(e, b, a)$ are real, which involves

$$(3.28) \quad \overline{\alpha_1} = \alpha_1, \quad \overline{\alpha_2} = \alpha_2.$$

Now let us fix $y, t \in \mathbb{R}$ and denote by h the function

$$(3.29) \quad h(y, t) = \frac{\Theta(\mathbf{Z} - \mathbf{d} + \frac{\mathbf{r}}{2})}{\Theta(\mathbf{Z} - \mathbf{d} - \frac{\mathbf{r}}{2})}.$$

By (3.12), x is a real-valued function of the real variables y and t if the function $\ln(h(y, t)) - \zeta$ is real, namely, if the function h is real and has a constant sign. From (2.22), (3.24) and (3.25) we deduce that

$$(3.30) \quad \overline{h(y, t)} = \frac{\Theta(\mathbf{Z} + \bar{\mathbf{d}} + \frac{\mathbf{r}}{2} + i\pi \operatorname{diag}(\mathbb{H}))}{\Theta(\mathbf{Z} + \bar{\mathbf{d}} - \frac{\mathbf{r}}{2} + i\pi \operatorname{diag}(\mathbb{H}))}.$$

Let us choose a vector $\mathbf{d} \in \mathbb{C}^g$ such that

$$\bar{\mathbf{d}} = -\mathbf{d} - i\pi \operatorname{diag}(\mathbb{H}) + 2i\pi \mathbf{T} + \mathbb{B}\mathbf{L}$$

for some vectors $\mathbf{T}, \mathbf{L} \in \mathbb{Z}^g$. Reality of the vector $\bar{\mathbf{d}} + \mathbf{d}$ together with (2.21) implies

$$(3.31) \quad \mathbf{d} = \frac{1}{2} \operatorname{Re}(\mathbb{B}) \mathbf{L} + i \mathbf{d}_I$$

for some $\mathbf{d}_I \in \mathbb{R}^g$, where the vectors \mathbf{T} and \mathbf{L} satisfy $2\mathbf{T} + \mathbb{H}\mathbf{L} = \operatorname{diag}(\mathbb{H})$. For this choice of the vector \mathbf{d} , (3.30) becomes

$$\overline{h(y, t)} = \frac{\Theta(\mathbf{Z} - \mathbf{d} + \frac{\mathbf{r}}{2})}{\Theta(\mathbf{Z} - \mathbf{d} - \frac{\mathbf{r}}{2})} \exp\{-\langle \mathbf{r}, \mathbf{L} \rangle\},$$

where we used the quasi-periodicity property (2.4) of the theta function. Therefore, the function h is real if $\mathbf{L} = 0$, that is $\mathbf{d} \in i\mathbb{R}^g$. Now let us check that h has a constant sign with respect to $y, t \in \mathbb{R}$. Since $\mathbf{Z} - \mathbf{d} \pm \frac{\mathbf{r}}{2} \in i\mathbb{R}^g$, by Proposition 2.2 the functions $\Theta(\mathbf{Z} - \mathbf{d} \pm \frac{\mathbf{r}}{2})$ of the real variables y and t do not vanish if the hyperelliptic curve is an M-curve, i.e., if all branch points in (3.1) are real. Hence h is a real continuous non vanishing function with respect to the real variables y and t , which means it has a constant sign. Therefore, x is a real-valued function of y and t if the constant ζ in (3.12) is chosen such that $\ln(h(y, t)) - \zeta$ is real. It is straightforward to see that the solution u (3.15) is a real-valued function of the real variables y and t , and then is real-valued with respect to the real variables x and t .

Now fix $t_0 \in \mathbb{R}$ and let us study smoothness conditions for the function $u(x, t_0)$ with respect to the variable x . First let us check that the solution u (3.15) is a smooth function of the real variable y . The function u is smooth with respect to y if and only if it does not have singularities. Since the theta function is entire, singularities of the solution u are located at the zeros of its denominator. By the same argument used previously to prove the real-valuedness of u , if the curve is an M-curve and $\mathbf{d} \in i\mathbb{R}^g$, the functions $\Theta(\mathbf{Z} - \mathbf{d} \pm \frac{\mathbf{r}}{2})$ and $\Theta(\mathbf{Z} - \mathbf{d})$ do not vanish. In this case, the function u is smooth with respect to the real variable y . Now let us prove that u is smooth with respect to the real variable x . By (3.12), the function $x(y)$ is smooth with respect to the variable y . Moreover, it can be seen from (3.12) and (3.7) that

$$(3.32) \quad x_y(y) = \frac{p_2}{g_1 g_2} = p_2 \frac{\Theta(\mathbf{Z} - \mathbf{d})^2}{\Theta(\mathbf{Z} - \mathbf{d} + \frac{\mathbf{r}}{2}) \Theta(\mathbf{Z} - \mathbf{d} - \frac{\mathbf{r}}{2})}.$$

Since the functions $\Theta(\mathbf{Z} - \mathbf{d} \pm \frac{\mathbf{r}}{2})$ and $\Theta(\mathbf{Z} - \mathbf{d})$ do not vanish, we deduce that $x(y)$ is a strictly monotonic real function, and thus the inverse function $y(x)$ has the same property. Therefore, the function $u(x, t_0) = u(y(x))$ is a smooth real-valued function with respect to the real variable x . \square

Now let us study real-valuedness and smoothness of the solutions in the case where $\tau a = b$.

Proposition 3.4. *Assume that all ramification points of \mathcal{R}_g are stable under τ and denote by $e \in \mathcal{R}_g(\mathbb{R})$ one of them. Let $a, b \in \mathcal{R}_g$ such that $\sigma(a) = b$ and assume that $\tau a = b$. Choose the local parameters such that $\overline{k_b(\tau p)} = k_a(p)$ for any point p in a neighborhood of a , and $\overline{k_e(\tau p)} = -k_e(p)$ for any p lying in a neighborhood of e . Denote by ℓ an oriented contour between a and b containing point e , which does not intersect cycles of the canonical homology basis. Assume that $\mathbf{N} = 2\mathbf{L}$ for some $\mathbf{L} \in \mathbb{Z}^g$, where $\mathbf{N} \in \mathbb{Z}^g$ is defined in (2.15). Take $k \in \mathbb{R}$ and define $\mathbf{d} = \mathbf{d}_R + \frac{i\pi}{2} \mathbf{N}$ for some $\mathbf{d}_R \in \mathbb{R}^g$. Choose $\zeta \in \mathbb{C}$ in (3.12) such that $\ln \left(\frac{\Theta(\mathbf{d} + \frac{\mathbf{r}}{2})}{\Theta(\mathbf{d} - \frac{\mathbf{r}}{2})} \right) - \zeta$ is real. Then solutions u (3.15) of the CH equation are real-valued. Moreover, for fixed $t_0 \in \mathbb{R}$, the function $u(x, t_0)$ is smooth with respect to the real variable x in the case where $\mathbf{N} = 0$, otherwise it has an infinite number of singularities of the type $O\left((x - x_0)^{\frac{2n}{2n+1}}\right)$ for some $n \in \mathbb{N} \setminus \{0\}$ and $x_0 \in \mathbb{R}$, which correspond to cusps.*

Proof. Analogously to the case where a and b are stable under τ , let us prove that solutions u (3.15) are real-valued. First let us check that the vector \mathbf{Z} (3.13) satisfies:

$$(3.33) \quad \overline{\mathbf{Z}} = \mathbf{Z}.$$

From (2.6) and (2.18) one gets $\overline{\mathbf{V}_a} = -\mathbf{V}_b$ and $\overline{\mathbf{V}_e} = \mathbf{V}_e$. Moreover, the vectors \mathbf{V}_a and \mathbf{V}_b satisfy $\mathbf{V}_a + \mathbf{V}_b = 0$ because of (3.8); thus we have $\overline{\mathbf{V}_b} = \mathbf{V}_b$ and $\overline{\mathbf{V}_e} = \mathbf{V}_e$ which proves (3.33). By (2.19) and (3.27) it can be deduced that α_1 and α_2 (3.14) satisfy

$$(3.34) \quad \overline{\alpha_1} = \alpha_1, \quad \overline{\alpha_2} = \alpha_2.$$

Moreover, from (2.18) and (2.15) one gets:

$$(3.35) \quad \overline{\mathbf{r}} = \mathbf{r} - 2i\pi\mathbf{N},$$

where $\mathbf{N} \in \mathbb{Z}^g$ is defined in (2.15). Now fix $y, t \in \mathbb{R}$. Let us check that x (3.12) is a real-valued function of the real variables y and t . By (3.34), this holds if the function h (3.29) is real and has a constant sign with respect to the real variables y and t . By (2.22),

(3.33) and (3.35) it follows that

$$(3.36) \quad \overline{h(y, t)} = \frac{\Theta(\mathbf{Z} - \bar{\mathbf{d}} + \frac{\mathbf{r}}{2} + \mathbf{p})}{\Theta(\mathbf{Z} - \bar{\mathbf{d}} - \frac{\mathbf{r}}{2} + \mathbf{p})},$$

where $\mathbf{p} = -i\pi\mathbf{N} - i\pi \operatorname{diag}(\mathbb{H})$. Let us choose the vector $\mathbf{d} \in \mathbb{C}^g$ such that

$$\bar{\mathbf{d}} \equiv \mathbf{d} + \mathbf{p} \pmod{2i\pi\mathbb{Z}^g + \mathbb{B}\mathbb{Z}^g},$$

which is, since $\bar{\mathbf{d}} - \mathbf{d}$ and \mathbf{p} are purely imaginary, equivalent to $\bar{\mathbf{d}} = \mathbf{d} + \mathbf{p} + 2i\pi\mathbf{T}$, for some $\mathbf{T} \in \mathbb{Z}^g$. Here we used the action (2.21) of the complex conjugation on the Riemann matrix \mathbb{B} , and the fact that \mathbb{B} has a negative definite real part. Hence, the vector \mathbf{d} can be written as

$$(3.37) \quad \mathbf{d} = \mathbf{d}_R + \frac{i\pi}{2}(\mathbf{N} + \operatorname{diag}(\mathbb{H}) - 2\mathbf{T}),$$

for some $\mathbf{d}_R \in \mathbb{R}^g$ and $\mathbf{T} \in \mathbb{Z}^g$. For this choice of the vector \mathbf{d} , by (3.36) the function h is a real-valued function of the real variables y and t . Now let us study in which cases the function h has a constant sign. The sign of the function h is constant with respect to y and t if the functions $\Theta(\mathbf{Z} - \mathbf{d} \pm \frac{\mathbf{r}}{2})$ do not vanish. By (3.33), (3.35) and (3.37), the vectors $\mathbf{Z} - \mathbf{d} \pm \frac{\mathbf{r}}{2}$ belong to the set S_1 introduced in (2.24). Hence by Proposition 2.1, the functions $\Theta(\mathbf{Z} - \mathbf{d} \pm \frac{\mathbf{r}}{2})$ do not vanish if the hyperelliptic curve is dividing (in this case $\operatorname{diag}(\mathbb{H}) = 0$), and if the arguments $\mathbf{Z} - \mathbf{d} \pm \frac{\mathbf{r}}{2}$ in the theta function are real (modulo $2i\pi\mathbb{Z}^g$). The vector $\mathbf{Z} - \mathbf{d} + \frac{\mathbf{r}}{2}$ is real if $\mathbf{T} = 0$ in (3.37). With this choice of the vector \mathbf{T} , the imaginary part of the vector $\mathbf{Z} - \mathbf{d} - \frac{\mathbf{r}}{2}$ equals $-i\pi\mathbf{N}$. Therefore, the vector $\mathbf{Z} - \mathbf{d} - \frac{\mathbf{r}}{2}$ is real modulo $2i\pi\mathbb{Z}^g$ if all components of the vector \mathbf{N} are even. To summarize, the function $h(y, t)$ defined in (3.29) is a real-valued function with constant sign if the hyperelliptic curve is dividing (i.e., all ramification points are stable under τ , since the ramification point e is stable under τ), if $\mathbf{T} = 0$ and $\mathbf{N} = 2\mathbf{L}$ for some $\mathbf{L} \in \mathbb{Z}^g$, where vector $\mathbf{N} \in \mathbb{Z}^g$ is defined in (2.15). Analogously to the proof of Proposition 3.3, we conclude that x is a real-valued continuous function of the real variables y and t , and thus solutions $u(x, t)$ (3.15) are real-valued functions of the real variables x and t .

Now let us study smoothness conditions for fixed $t_0 \in \mathbb{R}$. Notice that the function $u(y)$ (3.15) is a smooth function of the real variable y since the denominator does not vanish, as we have seen before. Put $\mathbf{z} = \mathbf{Z} - \mathbf{d}$. Let us consider the function $x_y(y)$ given in (3.32) in both cases: $\mathbf{N} = 0$ and $\mathbf{N} \neq 0$.

- If $\mathbf{N} = 0$, the function $x_y(y)$ does not vanish, since in this case $\mathbf{z} \in \mathbb{R}^g$ which implies that the function $\Theta(\mathbf{z})$ does not vanish. Hence, analogously to the case where a and b are stable under τ , for fixed $t_0 \in \mathbb{R}$, the function $u(x, t_0)$ is smooth with respect to the real variable x .

- If $\mathbf{N} \neq 0$, the function $\Theta(\mathbf{z})$ vanishes when \mathbf{z} belongs to the theta divisor. Fix $x_0, t_0 \in \mathbb{R}$ and denote by \mathbf{z}_0 and y_0 the corresponding values of \mathbf{z} and y . Assume that \mathbf{z}_0 is a zero of the theta function of order $n \geq 1$. Then by (3.32), the function $x_y(y)$ has a zero at y_0 of order $2n$. It follows that function $x(y) - x(y_0)$ has a zero of order $2n + 1$ at y_0 , and then

$$(3.38) \quad y(x) - y_0 = O\left((x - x_0)^{\frac{1}{2n+1}}\right).$$

On the other hand, it can be seen from (3.4) that

$$(3.39) \quad u_y(y) = p_2 \frac{\Theta(\mathbf{z})}{\Theta(\mathbf{z} + \frac{\mathbf{r}}{2}) \Theta(\mathbf{z} - \frac{\mathbf{r}}{2})} [\Theta(\mathbf{z}) \psi(\mathbf{z}) - 2D_b \Theta(\mathbf{z})],$$

where $\psi(\mathbf{z}) = D_b \ln \left(\Theta(\mathbf{z} + \frac{\mathbf{r}}{2}) \Theta(\mathbf{z} - \frac{\mathbf{r}}{2}) \right)$. Identity (3.39) implies that function $u_y(y)$ has a zero at y_0 of order $2n - 1$, namely,

$$(3.40) \quad u(y) - u(y_0) = O\left((y - y_0)^{2n}\right).$$

Finally with (3.38) and (3.40), the function $u(x, t_0)$ has an infinite number of singularities of the type $O\left((x - x_0)^{\frac{2n}{2n+1}}\right)$ which correspond to cusps. \square

4. NUMERICAL STUDY OF ALGEBRO-GEOMETRIC SOLUTIONS TO THE CAMASSA-HOLM EQUATION

In this section we will numerically study concrete examples for the CH solutions (3.15). As shown in the previous sections, real and bounded solutions are obtained on hyperelliptic M-curves, i.e., curves of the form

$$\mu^2 = \prod_{i=1}^{2g+2} (\lambda - \lambda_i),$$

where g is the genus of the Riemann surface, and where we have for the branch points $\lambda_i \in \mathbb{R}$ the relations $\lambda_i \neq \lambda_j$ for $i \neq j$.

For the numerical evaluation of the CH solutions (3.15) we use the code presented in [20, 21] for real hyperelliptic Riemann surfaces. The reader is referred to these publications for details. The basic idea is to introduce a convenient homology basis on the related surfaces, see Fig. 1. It is related to the basis used in the previous sections by the simple

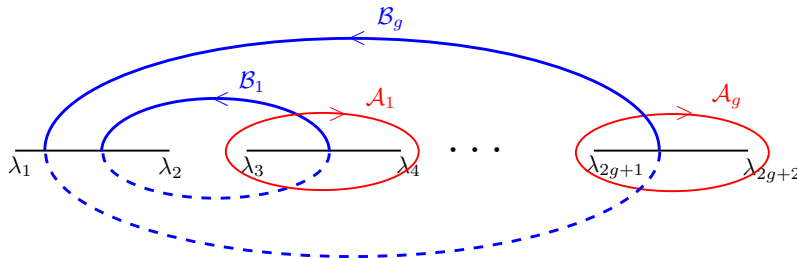


FIGURE 1. Homology basis on real hyperelliptic M-curves, contours on sheet 1 are solid, contours on sheet 2 are dashed.

relation $\mathcal{A} \rightarrow -\mathcal{B}$, $\mathcal{B} \rightarrow \mathcal{A}$. This choice of the homology basis has the advantage that the limit in which branch points encircled by the same \mathcal{A} -cycle collapse can be treated essentially numerically. Below we will consider examples where the distance of such a pair of branch points is of the order of machine precision (10^{-14}) and thus numerically zero. This limit is interesting since the \mathcal{B} -periods diverge, which implies that the corresponding theta functions reduce to elementary functions. The CH solutions (3.15) reduce in this case to solitons or cuspons. Since we want to study also this limit numerically, we use the homology basis of Fig. 1, and not the one of the previous sections.

The sheets are identified at the point a by the sign of the root picked by Matlab. We denote a point in the first sheet with projection λ into the complex plane by $\lambda^{(1)}$, and a point in the second sheet with the same projection by $\lambda^{(2)}$. The theta functions are in general approximated numerically by a truncated series as explained in [20] and [8]. A vector of holomorphic differentials for these surfaces is given by $(1, \lambda, \dots, \lambda^{g-1})^t d\lambda/\mu$. The periods of the surface are computed as integrals between branch points over these

differentials as detailed in [21]. The Abel map to the point a (and analogously for b) is computed in a similar way, see [25], as the integral between a and the branch point with minimal distance to a . It is well known (see for instance [7]) that the Abel map between two branch points is a half period.

To control the accuracy of the numerical solutions, we use essentially two approaches. First we check the theta identity (2.7), which is the underlying reason for the studied functions being solutions to CH. Since this identity is not implemented in the code, it provides a strong test. This computation for various combinations of the points a, b and e ensures that the theta functions are computed with sufficient precision, and that the quantities α_1 and α_2 in (3.12) are known with the wanted precision (we always use machine precision here). In addition, the smooth solutions are computed on Chebyshev collocation points (see, for instance, [28]) for x and t . This can be used to approximate the computed solution via Chebyshev polynomials, a so-called spectral method having in practice exponential convergence for smooth functions. Since the derivatives of the Chebyshev polynomials can be expressed linearly in terms of Chebyshev polynomials, a derivative acts on the space of polynomials via a so called differentiation matrix. With these standard Chebyshev differentiation matrices (see [28]), the solution can be numerically differentiated. The computed derivatives allow to check with which numerical precision the partial differential equation (PDE) is satisfied by a numerical solution. With these two independent tests, we ensure that the shown solutions are correct to much better than plotting accuracy (the code reports a warning if the above tests are not satisfied to better than 10^{-6}). We do not use the expansion in terms of Chebyshev polynomials for the cusped solutions since the convergence is slow for functions with cusps.

We first consider smooth solutions in the case $\tau a = a, \tau b = b$. To obtain non-trivial solutions in the solitonic limit, we use a vector \mathbf{d} corresponding to the characteristic $\frac{1}{2} \begin{bmatrix} 1 & \dots & 1 \\ 0 & \dots & 0 \end{bmatrix}^t$ in all examples. To plot a solution u in dependence of x and t , we compute it on a numerical grid for y and t to obtain $x(y, t)$ and $u(y, t)$. These are then used to obtain a plot of $u(x, t)$ without having to solve the implicit relation (3.12). In all examples we have $k = 1$. The solutions for $\tau a = b$, i.e., for points a and b on the cuts encircled by the \mathcal{A} -periods in Fig. 1 look very similar and are therefore not shown here.

Solutions on elliptic surfaces describe travelling waves and will not be discussed here. In genus 2 we obtain CH solutions of the form shown in Fig. 2. The typical soliton collision known from the KdV equation is also present here, the unchanged shape of the solitons after the collision, but an asymptotic change of phase.

In genus 6 the CH solutions have the form shown in Fig. 3. In the solitonic limit one can recognize a 6 soliton event.

The reality properties of the quantities entering the solution (3.15) depend on the choice of the homology basis. For instance, in the homology basis of Fig. 1 and for a and b stable under τ , the Abel map \mathbf{r} up to a vector proportional to $i\pi$ and the vectors $\mathbf{V}_b, \mathbf{V}_e$ are real, whereas these quantities are purely imaginary in the homology basis used in the previous sections. Thus the easiest way to obtain cusped solutions is in this case to put $e = \lambda_2$ and to choose \mathbf{d} corresponding to the characteristic $\frac{1}{2} \begin{bmatrix} 1 & \dots & 1 \\ 1 & \dots & 1 \end{bmatrix}^t$. It can be easily checked that the theta functions $\Theta(\mathbf{Z} - \mathbf{d} \pm \mathbf{r}/2)$ cannot vanish since the argument is real, whereas the $\Theta(\mathbf{Z} - \mathbf{d})$ will have zeroes since the argument is complex. This implies that the derivative u_x in (3.19) diverges which corresponds to cusps for the solution u . Peakons do not appear in such a limit of theta-functional solutions to CH and are thus not discussed here. To obtain them one would have to glue solutions in the solitonic limit on finite intervals to obtain a continuous solution that is piecewise C^1 .

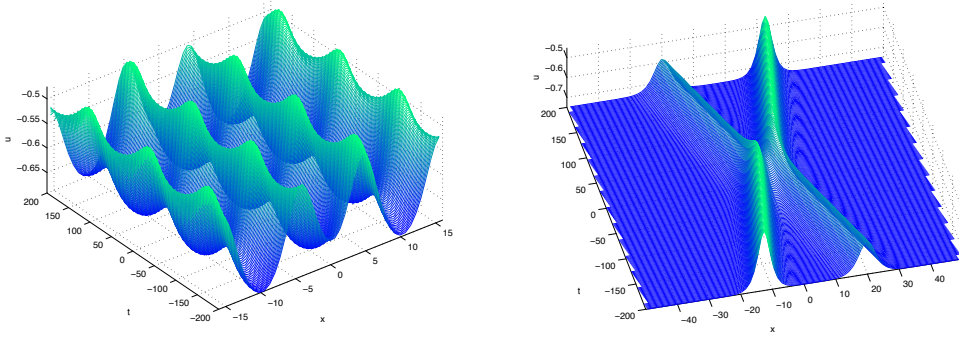


FIGURE 2. Solution (3.15) to the CH equation on a hyperelliptic curve of genus 2 with branch points $-3, -2, 0, \epsilon, 2, 2 + \epsilon$ and $a = (-4)^{(1)}$, $b = (-4)^{(2)}$ and $e = (-3, 0)$ for $\epsilon = 1$ on the left and $\epsilon = 10^{-14}$, the almost solitonic limit, on the right.

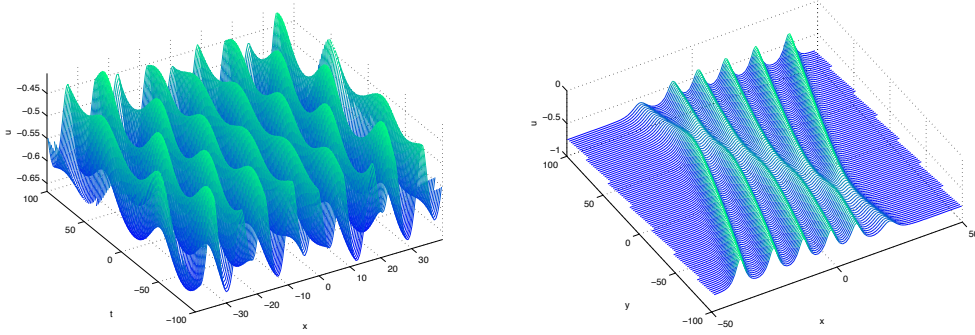


FIGURE 3. Solution (3.15) to the CH equation on a hyperelliptic curve of genus 2 with branch points $-7, -6, -5, -5 + \epsilon, -3, -3 + \epsilon, -1, -1 + \epsilon, 1, 1 + \epsilon, 3, 3 + \epsilon, 5, 5 + \epsilon$ and $a = (-8)^{(1)}$, $b = (-8)^{(2)}$ and $e = (-7, 0)$ for $\epsilon = 1$ on the left and $\epsilon = 10^{-14}$, the almost solitonic limit, on the right.

We show the cusped solutions always in a comoving frame $x' = x + vt$ to allow a better visualization of the solutions. In genus 2 we obtain cusped CH solutions of the form shown in Fig. 4, where also cusped solitons can be seen in the degenerate situation. Obviously the collision between cuspons is analogous to soliton collisions.

In genus 6 the CH solutions have the form shown in Fig. 5. In the solitonic limit one can recognize a 6-cuspon.

5. CONCLUSION

In this paper we have shown at the example of the CH equation that Mumford's program to construct algebro-geometric solutions to integrable PDEs can be also applied to non-local (here in x) equations. For the studied case the solutions in terms of multi-dimensional theta functions depend not directly on the physical coordinates x and t , but via an implicit

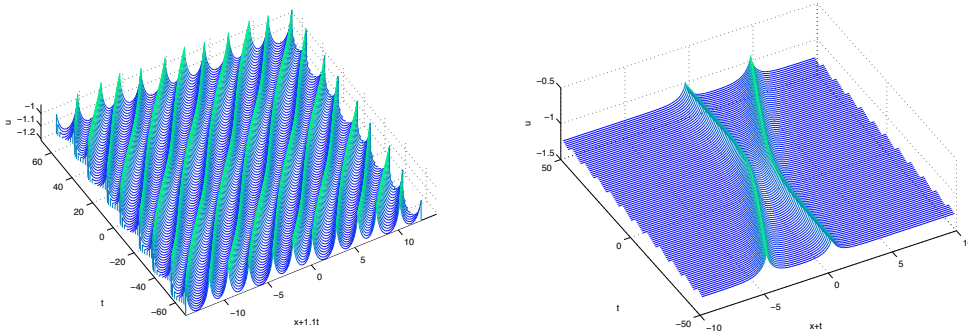


FIGURE 4. Cusped solution (3.15) to the CH equation on a hyperelliptic curve of genus 2 with branch points $-3, -2, 0, \epsilon, 2, 2 + \epsilon$ and $a = (-4)^{(1)}$, $b = (-4)^{(2)}$ and $e = (-2, 0)$ for $\epsilon = 1$ on the left and $\epsilon = 10^{-14}$, the almost solitonic limit, on the right.

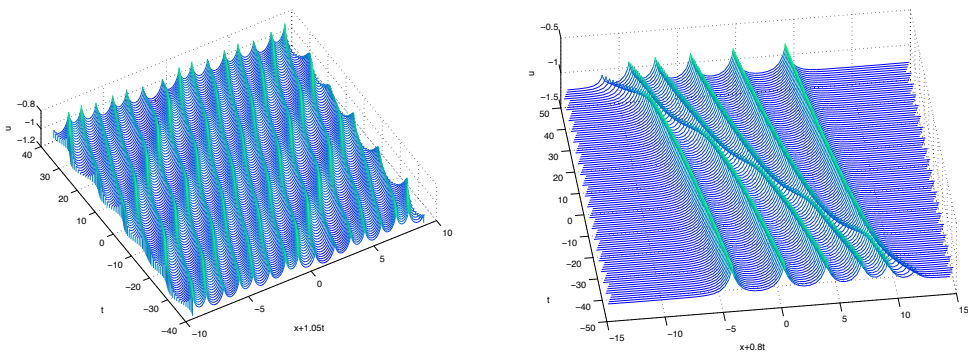


FIGURE 5. Solution (3.15) to the CH equation on a hyperelliptic curve of genus 6 with branch points $-7, -6, -5, -5 + \epsilon, -3, -3 + \epsilon, -1, -1 + \epsilon, 1, 1 + \epsilon, 3, 3 + \epsilon, 5, 5 + \epsilon$ and $a = (-8)^{(1)}$, $b = (-8)^{(2)}$ and $e = (-6, 0)$ for $\epsilon = 1$ on the left and $\epsilon = 10^{-14}$, the almost solitonic limit, on the right.

function. One consequence of this non-locality is the existence of non-smooth solitons. A numerical study of smooth and non-smooth solutions was presented.

A further example in this context would be the equation from the Dym-hierarchy for which theta-functional solutions were studied in [2], which will be treated elsewhere with Mumford's approach. It is an interesting question whether the 2+1 dimensional generalization of the CH equation [17, 14], for which algebro-geometric solutions are so far unknown, can be also treated with these methods.

REFERENCES

- [1] M.S. Alber, R. Camassa, F. Fedorov, N. Yu., D.D. Holm, J.E. Marsden, *The complex geometry of weak piecewise smooth solutions of integrable nonlinear PDE's of shallow water and Dym type*, Comm. Math. Phys. **221**, 197–227 (2001).
- [2] M.S. Alber, F. Fedorov *Wave solutions of evolution equations and Hamiltonian flows on nonlinear subvarieties of generalized Jacobians*, J. Phys. A **33**, 8409–8425 (2000).

- [3] M.S. Alber, F. Fedorov, N. Yu, *Algebraic geometrical solutions for certain evolution equations and Hamiltonian flows on nonlinear subvarieties of generalized Jacobians*, Inverse Problems **17**, 1017–1042 (2001).
- [4] W. Beals, D. Sattinger, J. Szmigielski, *Acoustic scattering and the extended Korteweg de Vries hierarchy*, Adv. Math. **140**, 190–206 (1998).
- [5] W. Beals, D. Sattinger, J. Szmigielski, *Multi-peakons and a theorem of Stieltjes*, Inverse Problems **15**, L1–L4 (1999).
- [6] W. Beals, D. Sattinger, J. Szmigielski, *Multipoleakons and the classical moment*, Adv. in Math. **154**, no. 2, 229–257 (2000).
- [7] E. Belokolos, A. Bobenko, V. Enolskii, A. Its, V. Matveev, *Algebro-geometric approach to nonlinear integrable equations*, Springer Series in nonlinear dynamics (1994).
- [8] A.I. Bobenko, C. Klein, (ed.), *Computational Approach to Riemann Surfaces*, Lect. Notes Math. **2013** (2011).
- [9] F. Calogero, *An integrable Hamiltonian system*, Phys. Lett. A **201**, 306–310 (1995).
- [10] F. Calogero, J.P. Francoise, *Solvable quantum version of an integrable Hamiltonian system*, J. Math. Phys. **37**, (6) 2863–2871 (1996).
- [11] R. Camassa, *Characteristic variables for a completely integrable shallow water equation*, In: Boiti, M. et al. (eds.) Nonlinearity, Integrability and All That: Twenty Years After NEEDS’79. Singapore: World Scientific (2000).
- [12] R. Camassa, D.D. Holm, *An integrable shallow water equation with peaked solitons*, Phys. Rev. Lett. **71**, (11) 1661–1664 (1993).
- [13] R. Camassa, D.D. Holm, J.M. Hyman, *A new integrable shallow water equation*, Adv. Appl. Mech. **31**, 1–33 (1994).
- [14] M. Chen, S. Liu, Y. Zhang, *A two-component generalization of the camassa-holm equation and its solutions*, Lett. Math. Phys. **75**, 1–15 (2005).
- [15] A. Clebsch, P. Gordan, *Theorie der Abelschen Funktionen*, Teubner, Leipzig (1866).
- [16] B.A. Dubrovin, S. Natanzon, *Real theta function solutions of the Kadomtsev-Petviashvili equation*, Math. USSR Investiya **32**:2, 269–288 (1989).
- [17] G. Falqui, *On a camassa-holm type equation with two dependent variables*, J. Phys. A: Math. Gen. **39** (2006).
- [18] J. Fay, *Theta functions on Riemann surfaces*, Lecture Notes in Mathematics **352** (1973).
- [19] A.S. Fokas, B. Fuchssteiner, *Symplectic structures, their Bäcklund transformations and hereditary symmetries*, Physica D **4**, 47–66 (1981/82).
- [20] J. Frauendiener, C. Klein, *Hyperelliptic theta functions and spectral methods*, J. Comp. Appl. Math. (2004).
- [21] J. Frauendiener, C. Klein, *Hyperelliptic theta functions and spectral methods: KdV and KP solutions*, Lett. Math. Phys., Vol. **76**, 249–267 (2006).
- [22] B.H. Gross, J. Harris, *Real algebraic curves*, Ann. sci. Ecole Norm. Sup. (4) **14**, 157–182 (1981).
- [23] A. Harnack, *Ueber die Vieltheiligkeit der ebenen algebraischen Curven*, Math. Ann. **10**, 189–199 (1876).
- [24] C. Kalla, *New degeneration of Fay’s identity and its application to integrable systems*, preprint arXiv:1104.2568v1 (2011).
- [25] C. Kalla and C. Klein, *On the numerical evaluation of algebro-geometric solutions to integrable equations* (2011) arXiv:1107.2108.
- [26] H.P. McKean, A. Constantin, *A shallow water equation on the circle*, Comm. Pure Appl. Math. Vol LII, 949–982 (1999).
- [27] D. Mumford, *Tata Lectures on Theta. I and II.*, Progress in Mathematics **28** and **43**, respectively. Birkhäuser Boston, Inc., Boston, MA (1983 and 1984).
- [28] L.N. Trefethen, *Spectral Methods in Matlab*, SIAM, Philadelphia, PA (2000).
- [29] V. Vinnikov, *Self-adjoint determinantal representations of real plane curves*, Math. Ann. **296**, 453–479 (1993).

INSTITUT DE MATHÉMATIQUES DE BOURGOGNE, UNIVERSITÉ DE BOURGOGNE, 9 AVENUE ALAIN
SAVARY, 21078 DIJON CEDEX, FRANCE

E-mail address: `Caroline.Kalla@u-bourgogne.fr`

INSTITUT DE MATHÉMATIQUES DE BOURGOGNE, UNIVERSITÉ DE BOURGOGNE, 9 AVENUE ALAIN
SAVARY, 21078 DIJON CEDEX, FRANCE

E-mail address: `Christian.Klein@u-bourgogne.fr`